Submitted to The Twenty-Eighth Symposium (International) on Combustion

Extinction Conditions of Nonpremixed Flames with Fine Droplets of Water and Water-NaOH Solutions

A.K. Lazzarini, R.H. Krauss, and **H.K. Chelliah**
Department of Mechanical and Aerospace Engineering
University of Virginia, Charlottesville, VA 22903

and

G.T. Linteris
Building and Fire Research Laboratory
National Institute of Standards and Technology, Gaithersburg, MD 20899

Subject:	Fire Research	
Corresponding author:	Dr. H.K. Chelliah Department of Mechanical and Aerospace Engineering University of Virginia Charlottesville, VA 22903 Phone: (804) 924-6037 Fax: (804) 982-2037 E-mail: harsha@virginia.edu	
Word Count:	Text + References:	3970 words
	1 Table + 6 Figures:	1400 words
	Total:	5370 words
Presentation:	Oral	

Extinction Conditions of Nonpremixed Flames with Fine Droplets of Water and Water-NaOH Solutions

A.K. Lazzarini, R.H. Krauss, H.K. Chelliah
Department of Mechanical and Aerospace Engineering
University of Virginia, Charlottesville, VA 22903, USA
and
G.T. Linteris
Building and Fire Research Laboratory
National Institute of Standards and Technology, Gaithersburg, MD 20899, USA

Interactions of fine droplets of water and water-NaOH solutions with a steady, laminar counterflow methane-air nonpremixed flame are investigated, both experimentally and numerically. A water atomizer generating a polydisperse distribution of droplet sizes with a median diameter of 20 μm is used in experiments with steady feed rate. Comparisons of the measured flame extinction condition as a function of droplet mass fraction in the air stream indicate a trend similar to that predicted previously using 20 μm monodisperse water droplets. The hybrid Eulerian-Lagrangian numerical model previously developed is generalized to include polydisperse distribution of drop sizes, however, the differences seen between experiments and the numerical predictions at high water mass fractions could not be attributed to variation in size distribution alone. Present experiments support the conclusions of an earlier modeling work that, on a mass basis, fine water mist can be as effective as the now banned gaseous fire suppressant halon 1301. Inclusion of NaOH in water (up to 18% by mass), is shown to significantly enhance the fire suppression ability of water by complementing its thermal effects with chemical catalytic radical recombination effects of NaOH.

INTRODUCTION

On a mass basis, water is known to be a very effective fire suppressant. In particular, water in the form of a fine mist (i.e. drop sizes below 100 μm), with relatively long settling times under normal gravity conditions, can be an excellent suppressant for gaseous fires in enclosures where total flooding is typically required. Such fires have been previously suppressed using halon 1301, but the production of halon 1301 has been banned because of its adverse effects on the ozone layer [1]. Irrespective of the specific application, detailed quantitative information regarding the fundamental fire suppression mechanism of water mist is useful in order to select types of applications and delivery methods, and also to explore methods of enhancing the fire suppression ability of water mist (eg. through chemical additives). This paper presents such a basic investigation using a counterflow nonpremixed flow configuration, with detailed comparisons between experiments and modeling.

Basic investigations aimed at better understanding the fire suppression mechanism of water dates back to 1950's [2], while more recent studies have focused primarily on water-mist systems [4-8]. Although there is a consensus in the literature on the fundamental fire suppression mechanism of water, no detailed quantitative information on the various physical, thermal and chemical effects of water-mist were available until recent modeling capabilities were developed. The detailed modeling efforts were primarily carried out in two configurations, counterflow [5, 6] and co-flow [7]. The former flow configuration provides a convenient approach in understanding the interactions between droplet dynamics with flames, including flame extinction conditions [9-11]. For example, investigations by Lentati and Chelliah [5] have shown that dilution of the air stream (or displacement of oxygen) with saturated water vapor alone reduces the extinction strain rate of a methane-air nonpremixed flame by about 12%. Experimental data are presented for the first time in this paper to support such predictions. Further addition of water, in the form of fine droplets, causes significant thermal cooling of the flame front because of the relatively large latent heat of vaporization of water. For example, addition of 3% of water by mass in the form of 20 μm monodisperse droplets (the optimum size for this flow configuration) were shown to reduce

the extinction strain rate by an additional 55% [5]. By selectively excluding the source terms contributing to the gas-phase and the condensed phase conservation equations, the importance of thermal effects associated with water-mist were clearly demonstrated [6]. The chemical and other physical effects associated with fine-water droplets were shown to have a minor effect.

For a given mass fraction of water in condensed phase, previous predictions with monodisperse droplets have shown an increase in the flame extinction strain rate when droplet sizes are either below or above 20 μm, indicating a nonmonotonic effect on flame suppression as a function of droplet size [5]. Another significant finding in these initial counterflow numerical studies is that, on a mass basis, 20 μm water droplets are equally as effective in suppressing counterflow flames as the chemical suppressant halon 1301 [6]. Since these numerical studies were not supported by any experimentation or analytical results, the experiments described here were undertaken to validate such predictions. In practice, however, steady introduction of monodisperse size droplets was found to be a rather difficult task. Although efforts are still underway to achieve this goal, the results presented here used a polydisperse atomizer (described below), for which the size dsitribution was measured using a phase-Doppler particle analyzer (PDPA) available at NIST. The previously developed hybrid Eulerian-Lagrangian numerical model [5] for monodisperse water droplet sizes is generalized here to account for such polydisperse size distributions of water droplets. The predicted results with these polydisperse size distributions are shown to be consistent with previous monodisperse predictions, however differences observed between experiments and modeling could not be explained solely on the basis of the size distribution effects.

In addition to pure water-mist results, experimental flame extinction results with water-NaOH solutions are also presented for the present counterflow nonpremixed methane-air flame. The significant enhancement in flame suppression ability of water-NaOH solutions (almost a factor of five for 18% of NaOH by mass in water) is found to be consistent with previous experiments reported by Zheng et al. [4] for premixed counterflow flames using water-NaCl solutions.

EXPERIMENTAL METHOD

Counterflow Burner

In experiments, a steady, planar, nonpremixed flame established within the mixing layer of a counterflow of methane and air was employed. Figure 1 shows a schematic of the experimental setup of the counterflow burner, in which the fuel and air nozzles shown are made from Pyrex glass. The exit diameter of the annular part of the tubes is 15 mm with a nozzle area contraction factor of 6.5, producing a nearly plug flow velocity profile at the nozzle exit. The co-annular nitrogen streams on both fuel and air sides help maintain a very stable planar flame disk. The cylindrical burner chamber includes provision for dilution of the chamber with room air at the bottom (to minimize the occurrence of secondary flames), water cooling, and easy adjustment of the nozzle separation distance with MDC vacuum fittings. The typical separation distance between the two nozzles is between 10-12 mm. The exhaust gases were evacuated using an air-driven mass flow ejector, with the chamber pressure monitored by a differential pressure gauge. The air was supplied by an oil-free compressor and was dried by passing through a series of dessicants. The methane used was BOC grade 4.0 with a purity of 99.99%. The flow rates of fuel and air were controlled using factory-calibrated Teledyne Hastings-Raydist mass flow meters, with reported accuracy of +/-1%.

For experiments involving water vapor and droplets, the metered dry air was saturated before it entered the vertical Pyrex air tube by passing it through a porous tube submerged in a water flask. Heating the water flask to about 1-5 ^{o}C above the room temperature was found to facilitate saturation of air to >99% relative humidity. There was no detectable increase in air temperature above the room temperature because the long connecting tube allowed sufficient time to attain thermal equilibrium with the surroundings. The droplet atomizer was located at the bottom of the vertical Pyrex air nozzle such that the droplets were uniformly dispersed at the nozzle exit. This uniformity of droplet size distribution was characterized using the PDPA. The Pyrex tube proved to be very useful in observing the droplet condensation on the inner walls.

Droplet Generation

Two types of droplet generators were used, (a) piezoelectrically excited fluid jet atomization system acquired from Fluid Jet Associates [12] and (b) ultrasonic fluid surface breakup system acquired from Sono-Tek. The first atomizer is capable of generating truly monodisperse droplets, but this system used very narrow orifices (eg. 10μm hole generating $\sim 20\mu$m droplets) that proved susceptible to clogging and erosion problems. By varying the plate orifice diameter, this atomizer could be used to generate different monodisperse drop sizes. The second atomizer from Sono-Tek was found to be relatively simple to implement and was free of the operational problems of the Fluid Jet atomizer, but the droplets generated had a relatively wide size distribution. The median droplet size of the ultrasonic atomizer could be varied by selecting a different nozzle tip length and resonance frequency. All of the experimental flame extinction data presented in this paper were obtained using this Sono-Tek atomizer.

The Sono-Tek droplet generation system consists of an ultrasonic nozzle and the Sono-Tek Broadband Ultrasonic Generator. A syringe pump (Instech Model 2000), fitted with a plastic Becton Dickinson 10cc syringe was used to feed water to the atomizer. For a fixed water mass flow rate, the air and fuel flows were increased until the flame extinguished. The flame was found to be very stable until the extinction point.

The method of calibrating the droplet mass flow rate is extremely important for data validation. The calibration was performed using a container 75 mm in diameter and 35 mm in height with a plastic lid that sealed tightly onto the end of the air nozzle. The damp cotton inside the container provided a tortuous path to trap the droplets and ensured that the air left the container still saturated (if the relative humidity of the air decreased as it passed through the container, the measured droplet flowrate would appear to vary in time and result in a water droplet mass flow rate higher than the actual value). The air escaped the container through holes that were punched in the top of the container. Before and after each flame extinction experiment, the air-side burner was lowered to where the calibration cup could be attached. Calibration was performed in the same manner for both pure water

and water-NaOH cases.

Droplet Size Distribution

The droplet size distribution in the vicinity of the Sono-Tek atomizer nozzle has been characterized by the manufacturer and is known to follow a log-normal distribution, with a median diameter of about 20 μm and a Sauter mean diameter (SMD) of about 30 μm. This normalized distribution, separated into twelve discrete sections for modeling purposes, is shown in Fig. 2a. Based on the estimated settling velocities of different drop sizes, for typical flow velocities in the air tube, it was found that not all the drops were convected out of the air nozzle. For example, for air flow rate corresponding to a flow strain rate of about 285 s^{-1}, the estimated maximum drop size that could be carried in the air stream was about 75 μm, while for a strain rate of 160 s^{-1} the corresponding maximum drop size was about 55 μm. These estimates and the quality of the air-droplet flow leaving the air nozzle was verified using the PDPA. Figure 2b shows the measured drop size distribution for a high strain rate of 285 s^{-1} and Fig. 2c shows a similar plot for a lower strain rate of 160 s^{-1}. The shift in maximum size of droplets is consistent with estimated values, while the general shape of the distribution still retains the log-normal shape.

EXPERIMENTAL EXTINCTION RESULTS

With the counterflow burner described above, flame extinction experiments were conducted by increasing the air and methane nozzle exit velocities such that the momentum of the two streams were balanced, i.e. $(\rho v^2)_{air} = (\rho v^2)_{CH_4}$, where ρ is the density and v is the axial velocity. Knowing the nozzle separation distance, L, the flow strain rate is defined by the global formula $a = 4|v_{air}|/L$ [13]. For nonpremixed methane-air flames, the measured global flame extinction strain rate of 470 s^{-1} was obtained, while the measured local flow velocity using a laser Doppler velocimetry (LDV) system yielded a local flow strain rate of about 390 s^{-1}. Both of these numbers were highly reproducible and consistent with previous experiments and modeling efforts [14]. The experimental flame extinction results presented

in this paper are all based on the global strain rate formula, unless otherwise mentioned.

Water Vapor

The presence of condensed-phase water implies that the air stream is saturated with water vapor. At atmospheric pressure and room temperature of 300 K, the saturated water vapor mole fraction in air is 3.51% (or mass fraction Y_{vap}=0.0224). This saturated water vapor can have a significant effect on the flame extinction condition, mainly through the displacement of oxygen. Previously, detailed modeling efforts have indicated that the predicted local flame extinction strain rate can reduce from 420 s^{-1} for a methane-air flame to 365 s^{-1} for methane and air saturated with water vapor (a reduction in extinction strain of 12%) [5]. Present experiments with saturated water vapor in the air stream have yielded a global extinction strain rate of 405 s^{-1} (a reduction of 13% from 470 s^{-1}), indicating an excellent agreement with the predictions.

Pure Water Droplets

The ultrasonic atomizer described above with a median drop diameter of about 20 μm is employed here to investigate interactions between water droplets and the nonpremixed laminar methane-air flame. With increasing droplet number density (or mass fraction of water droplets in the air stream), it is expected that the flame extinction will occur more easily, resulting in a lower extinction strain rate. Figure 3 indicates such a plot where the mass fraction of water in condensed phase (Y_0) is plotted as a function of the flame extinction strain rate. Note that the zero water droplet mass fraction corresponds to the case where the air stream is saturated with water vapor (i.e. $Y_{vap} = 0.024$). In this figure, the symbols are from experiments with the extinction strain rate determined from the global formula. Also shown in Fig. 3 are the predicted variations of water droplet mass fraction as a function of global (solid line) and local (dashed line - calculated based on the velocity gradient dv/dx near the oxidizer boundary of the mixing layer) extinction strain rates, assuming 20 μm monodisperse droplets. Irrespective of the assumption of monodisperse drop size distribution

in simulations, the predicted trend is seen to be in close agreement with experiments.

Although the experiments and predictions agree well for pure water vapor, with increasing droplet mass loading, the differences become rather large. In predictions, relaxation of the monodisperse size distribution approximation based on the measured distributions shown in Fig. 2 is not expected to rectify this difference because 20 μm monodisperse droplets have been predicted to be the most effective. As discussed later in the numerical section, any broadening of the size distribution about 20 μm leads to higher mass fraction of water in condensed phase for the same flame extinction condition. Thus, differences seen in Fig. 3 between experiments and modeling are likely be due to other causes. In experiments, calibration of the water droplet mass flow rate through gravimetric analysis can introduce errors, however, considerable care was taken to address uncertainties associated with the approach adopted.

Water with NaOH

The primary mechanism of flame extinction by fine water droplets is through the thermal cooling of the flame front leading to slower chemical reaction rates. For example, in a counterflow field of methane and air, the 20 μm droplets were shown to be most effective because most of the droplet mass is predicted to evaporate near the oxygen consumption or radical species production region [15, 16]. This thermal effect of water droplets can be considerably enhanced by including a chemically active fire suppressing compound in water. NaOH is selected as it known to be the primary compound in the catalytic radical recombination path of sodium bicarbonate fire suppression [17]). Since the solubility of NaOH in cold water is about 30% of the total mass [18], a significant amount of NaOH can be released at the flame front, provided that the fine droplets consisting of water-NaOH are completely vaporized. Here, the same Sono-Tek atomizer with median drop size of 20 μm was used to deliver various solutions of water-NaOH and investigate their effect on suppressing counterflow methane-air flames.

Figure 4 shows a plot comparing the experimentally measured water-NaOH mass fractions

as a function of the flame extinction strain rate. As before, the air flowing into the nozzle tube was saturated with pure water vapor. Because the NaOH vapor pressure is very small ($<$ 1 mmHg at room temperature [18]), air saturated with pure water vapor is not expected to affect the evaporation of NaOH. The measured results indicate that with increasing NaOH mass fraction in water, the amount of water-NaOH mass fraction needed for flame extinction decreased significantly; almost a factor 5 for 18% NaOH by mass in water at the lowest strain rate considered. The concept of combining thermal and chemical effects could lead to a significant increase in fire suppression ability, as shown in Fig. 4.

NUMERICAL PREDICTIONS

Effect of a Constant Mass Flow Rate of Water

As described in the experimental section, in these two-phase experiments, the flame extinction was realized by increasing the flow rate of methane and air (saturated with water vapor), while the mass flow rate of condensed water droplets ($\dot{m}_{H_2O,c}$) was held constant by the syringe pump. During this process, the mass fraction of water droplets ($Y_0 = \dot{m}_{H_2O,c}/[\dot{m}_{air} + \dot{m}_{H_2O,c}]$) in air changed because of the varying air mass flow rate ($\dot{m}_{air}$). In previous numerical predictions, it was assumed that condensed phase water mass fraction (Y_0) was held constant at all strain rates. The predicted flame temperature variation as a function of flow strain rate, for constant $\dot{m}_{H_2O,c}$ and for constant Y_0 are shown in Fig. 5, for 20 μm monodisperse droplets. In the absence of radiative losses, usually only one extiction condition is realized for constant Y_0. Instead, if experiments are performed with constant $\dot{m}_{H_2O,c}$=2.65 mg/s/cm^2 (inner most closed oval in Fig. 5) and started at some strain rate away from extinction (say point P), then theoretically two flame extinction points can be attained, depending on whether strain rate is increased (point E1) or strain rate is decreased (point E2) by varying only the air and fuel flow rates in a proportional manner to keep the momentum balanced. This phenomenon is purely a consequence of the two-phase system considered and its occurrence was observed for water-NaOH solutions. In practice, this second extinction point (E2) can be realized by decreasing the oxidizer transport while the

droplet transport is held constant.

Effect of Polydispersivity

The model developed previously to simulate the interaction of fine water droplets with gaseous flames was based on a hybrid Eulerian-Lagrangian formulation for the gas and condensed phase [5]. In this model, the Lagrangian description of the water droplet transport was based on a monodisperse size of droplets. This assumption certainly made the computations less demanding, but more importantly, the analyses of the results on droplet size effects became considerably simpler. Because of the experimental difficulties in realizing truly monodisperse water droplet distributions, the above model is generalized here to include the polydisperse size effects. It was shown previously that for water mass loadings similar to those considered here, the ratio of droplet-to-droplet separation distance to droplet size was over 20. Under such conditions, the equation for droplet mass flux ($\mathcal{F}$) (i.e. the spray equation), written in the form for the present quasi-one dimensional counterflow field [5]

$$\frac{d\mathcal{F}}{dt} + 2\mathcal{F}U_d = \Gamma,$$

can be simplified by setting the droplet collision source term, $\Gamma = 0$. Thus, by treating the droplet size distribution as composed of several discrete size groups [19, 20], the simulation simplifies to solving several Lagrangian equations for these discrete drop size groups, with initial conditions corresponding to each discrete size group specified at the air nozzle exit.

For 1% mass fraction of water in condensed phase, flame extinction calculations were performed with the three different discrete polydisperse size distributions shown in Fig. 2. A comparison of these flame extinction results with the ideal 20 μm drop size for this flow configuration is shown in Table 1. The predicted extinction strain rates indicate that any broadening of the size distribution of droplets from the ideal 20 μm size leads to a higher flame extinction strain, and to deviate further from the experiments. At higher water mass loadings and decreasing flow strain rates, the thermal radiation effects are known to increase, and may also have an influence in the present predictions. However, the strain rates indicated

in Table 1 are rather moderate and it is very unlikely that the significant differences between experiments and modeling can be solely attributed to the radiation heat loss effects. Thus, the underlying cause for the differences seen is perhaps due to the quasi-one dimensional formulation or analytical models employed for the droplet evaporation and heating, and all of these issues must be addressed in the future.

CONCLUSIONS

The main purpose of the present work was to provide experimental data to validate the recent numerical predictions on the effectiveness of fine-water droplets in extinguishing counterflow nonpremixed flames. On a mass basis, the predicted ability of fine water-mist to suppress gaseous fires with similar or better effectiveness than halon 1301 was verified. Although the original goal was to obtain results using monodisperse size fine droplets as assumed in previous theoretical investigations, this task became rather challenging for many practical reasons. Instead, an ultrasonic water atomizer generating log-normal distribution of drop sizes, with median drop size of about 20 μm was employed. The actual droplet size distribution was expected to deviate from the prescribed distribution at the atomizer depending on the convective velocity in the air tube in the counterflow burner, and this variation was characterized using a PDPA. The hybrid Eulerian-Lagrangian numerical model was extended to include such polydisperse droplet size distributions, subject to the assumption that the droplet collisions are negligible based on the large separation distance between droplets compared to their diameter.

When the air stream is saturated with water vapor only, it was shown that the counterflow nonpremixed flame extinction condition measurements agreed extremely well with the corresponding numerical predictions. With addition of condensed phase water droplets the trends agreed well, however, considerable differences do exist between the experiments and modeling. The observed differences were shown to be mildly affected by the polydispersivity of the atomizer employed. This led to the conclusion that other submodels in the numerical model, including radiative heat losses, need to be evaluated.

Addition of a chemically active fire suppressing compound to water, namely NaOH, was shown to complement the thermal fire suppression mechanism of water. At the low end of the strain rates investigated ($\sim 125\ s^{-1}$), 18% by mass of NaOH in the solution was shown to reduce the flame extinction strain rate by almost a factor of five. Although inclusion of NaOH may not be desired in many practical applications because of its corrosive effects, the concept of combining the thermal and chemical effects of these condensed phase agents may lead to the development of superior fire suppressants.

Acknowledgment: This work is supported by National Institute of Standards and Technology, Gaithersburg, MD, through grant No. HH0095.

References

[1] Grosshandler, W.L., Gann, R.G., and Pitts, W.M., *Evaluation of Alternate In-Flight Fire Suppressants for Full-Scale Testing in Aircraft Engine Nacelles and Dry Bays*, NIST SP-861, April, 1994.

[2] Rabash, D.J., Rogowski, Z.W., and Stark, G.W.V., *Combust. and Flame* **4**:223-234 (1960).

[3] Mawhinney, J.R., Dlugogorski, B.Z., and Kim, A.K., *Fire Safety Sci.*, Proceedings of the Fourth Int. Symposium, pp. 47-60, 1994.

[4] Zheng, R., Bray, K.N.C., and Rogg, B., *Combust. and Flame* **126**:389-401 (1997).

[5] Lentati, A.M. and Chelliah, H.K., *Combust. and Flame*, **115**:158-179 (1998).

[6] Lentati, A.M. and Chelliah, H.K., *Twenty-Seventh (Int.) Symposium on Combustion*, The Combustion Institute, Pittsburgh, pp. 2839-2846, 1998.

[7] Prasad, K., Li, C., Kailasanath, K., Ndubizu, C., Ananth, R., and Tatem, P., *Combust. Sci. and Tech.* **132**:325-364 (1998).

[8] Zegers, E.J.P., Williams, B.A., Sheinson, R.S., and Fleming, J.W., "Water mist suppression of non-premixed counterflow flames," *Eastern States Section*, The Combustion Institute, Raleigh, NC, Oct. 1999.

[9] Continillo, G. and Sirignano, W.A., *Combust. and Flame* **81**:325 (1990).

[10] Lacas, F., Darabiha, N., Versaevel, P., Rolon, J.C., and Candel, S., *Twenty-Fourth Symposium (Int.) on Combustion*, The Combustion Institute, p. 1523, 1992.

[11] Chen, N.-H., Rogg, B., and Bray, K.N.C., *Twenty-Fourth Symposium (Int.) on Combustion*, The Combustion Institute, p. 1513, 1992.

[12] Takahashi, F., Schmoll, W.J., and J.L. Dressler, J.L., *Rev. Sci. Instrum* **65**(11), pp. 3563-3569 (1994).

[13] Seshadri, K. and Williams, F.A., *Int. J. Heat Mass Transfer* **21**, 251 (1978).

[14] Chelliah, H.K, Law, C.K., Ueda, T., Smooke, M.D., and Williams, F.A., *Twenty-third Symposium (Int.) on Combustion*, The Combustion Institute, p. 503, 1990.

[15] Seshadri, K. and Peters, N., *Combust. and Flame* **73**:23 (1988).

[16] Chelliah, H.K. and Williams, F.A., *Combust. and Flame* **60**:17 1990.

[17] Jensen, D.E. and Jones, G.A., *J. Chem. Soc., Faraday Trans. Part I* **78**, p. 2843, 1982.

[18] Weast, R.C., Astle, M.J, and Beyer, W.H., *CRC Handbook of Chemistry and Physics* (65th ed), CRC Press, Boca Raton, FL, 1985.

[19] Greenberg, J.B., Silverman, I., and Tambour, Y., *Combust. and Flame* **93**:90-96 (1993).

[20] D'Angelo, Y., Silverman, I., Gao, L.P., Gomez, A., and Smooke, M.D., "Computational and Experimental Study of Counterflow Spray Diffusional Flames," Eastern-State Section, The Combustion Institute, Hilton Head, SC, Dec. 1996.

Table and Figure Captions

Table 1 Comparison of the flame extinction strain rate for different size distributions of water droplets.

Figure 1: Schematic of the counterflow burner configuration with the water droplet atomizer.

Figure 2a: The normalized droplet size distribution of the Sono-tek atmozier as reported by the manufacturer, divided into 12 discrete sections.

Figure 2b: The normalized water droplet size distribution measured using a PDPA at the exit of the air nozzle, for an air flow rate corresponding to a counterflow strain rate of 285 s^{-1}.

Figure 2c: The normalized water droplet size distribution measured using a PDPA at the exit of the air nozzle, for an air flow rate corresponding to a counterflow strain rate of 160 s^{-1}.

Figure 3: Variation of water droplet mass fraction in condensed phase as a function of flame extinction strain rate, symbols from experiments and lines from predictions.

Figure 4: Comparison of the droplet mass fraction in condensed phase as a function of flame extinction strain rate, for different mass loadings of NaOH in water.

Figure 5: The variation of the maximum flame temperature as a function of local flow strain rate, for constant droplet mass fractions (lines) and for constant water mass flux rates (lines with symbols).

Table 1: A comparison between the experimental and predicted global flame extinction strain rate (s^{-1}), for different drop size distributions with the same water droplet mass fraction of 1%.

	Experiments	20μm monodisperse droplets	Distribution from Fig. 2a	Distribution from Fig. 2b	Distribution from Fig. 2c
Global strain rate	180	286	297	291	292

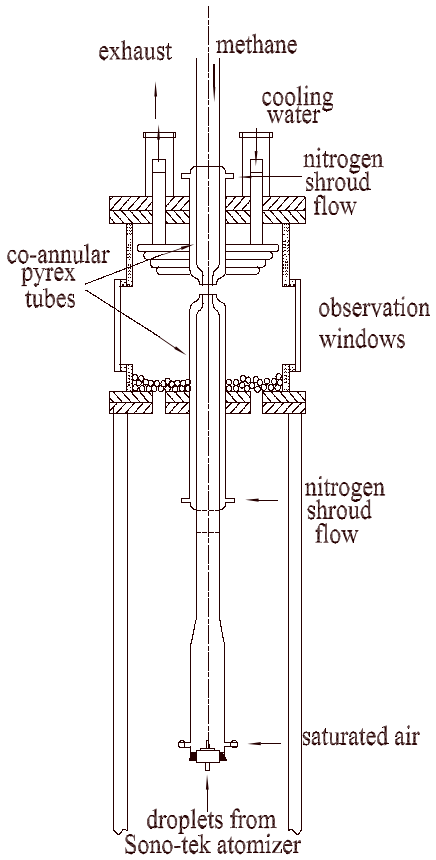
exhaust
methane
cooling water
nitrogen shroud flow
co-annular pyrex tubes
observation windows
nitrogen shroud flow
saturated air
droplets from Sono-tek atomizer

Figure 1

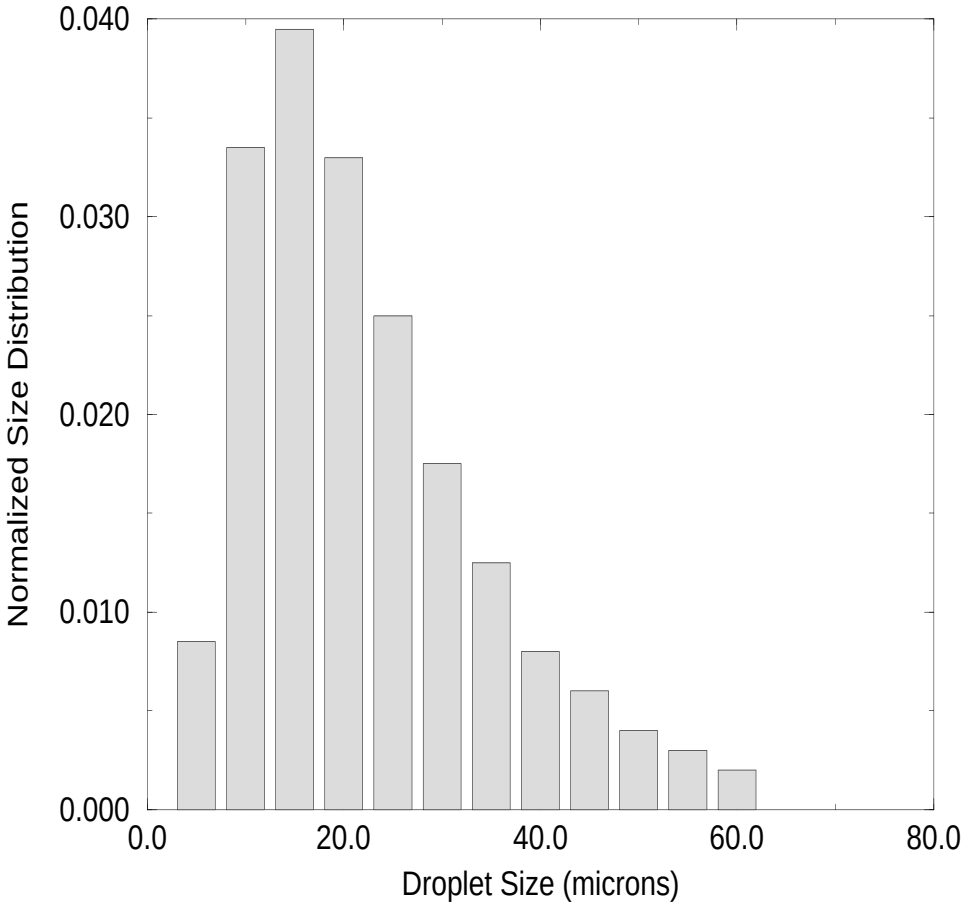
0.040
0.030
0.020
0.010
0.000
Normalized Size Distribution
0.0
20.0
40.0
60.0
80.0
Droplet Size (microns)

Figure 2a

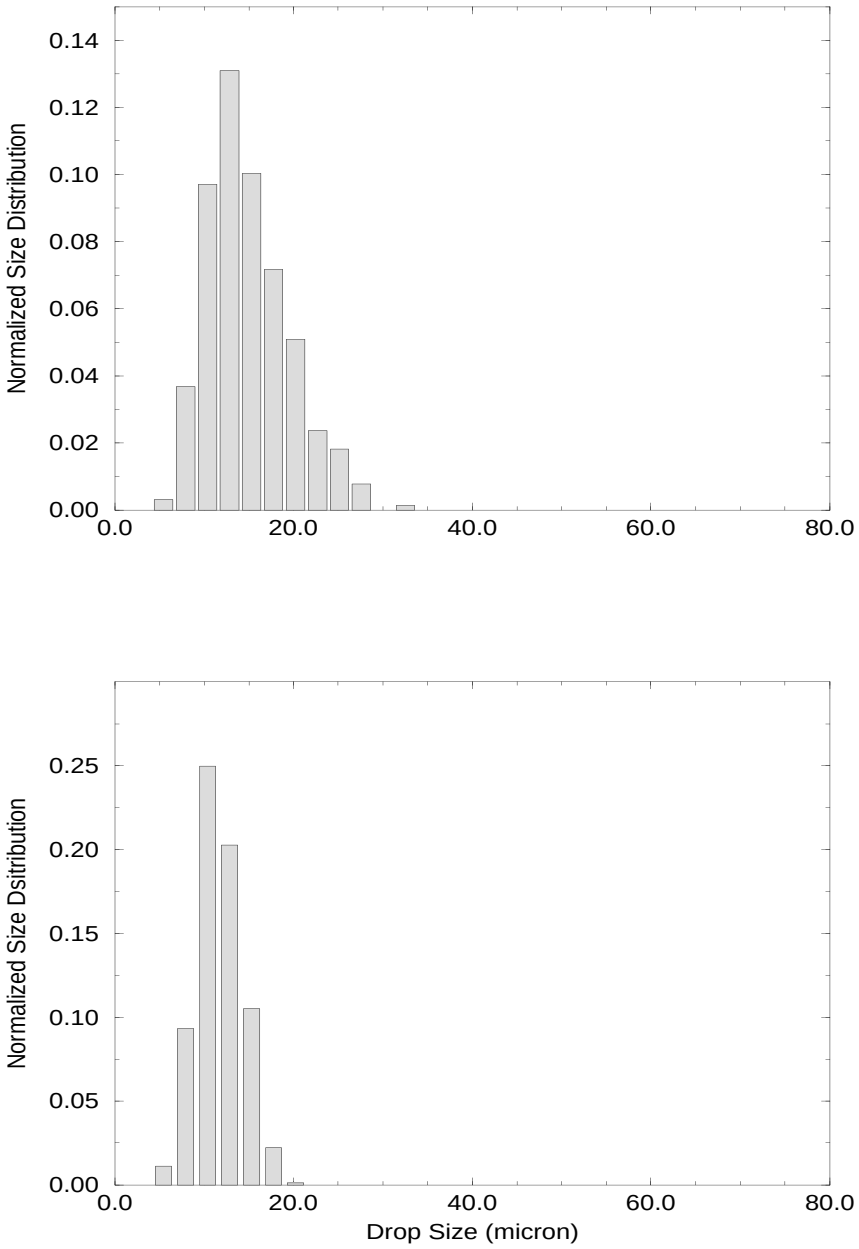

Figure 2b and 2c

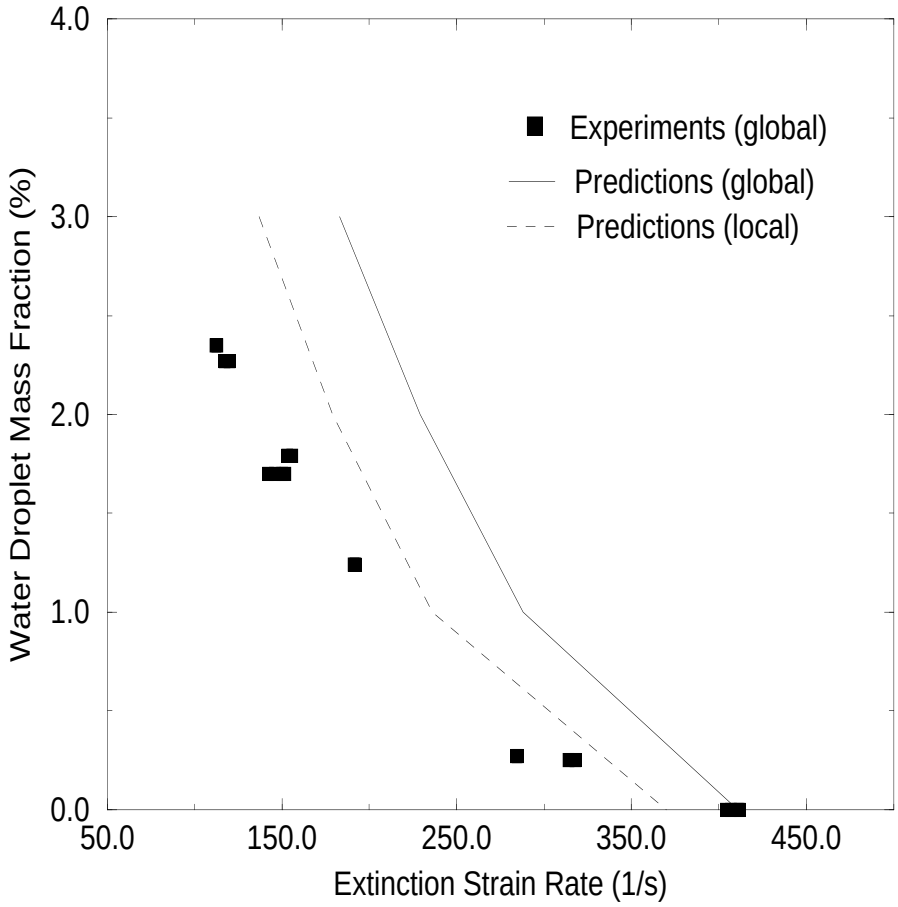
4.0
3.0
2.0
1.0
0.0
50.0
150.0
250.0
350.0
450.0
Water Droplet Mass Fraction (%)
Extinction Strain Rate (1/s)
Experiments (global)
Predictions (global)
Predictions (local)

Figure 3

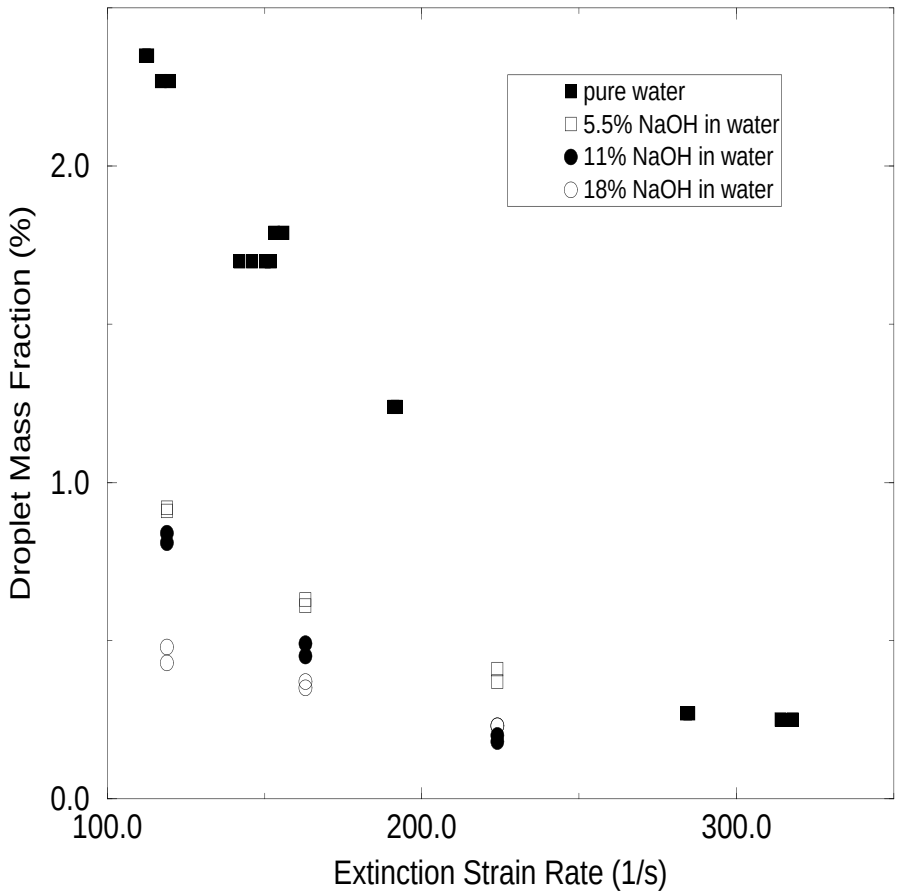
pure water
5.5% NaOH in water
11% NaOH in water
18% NaOH in water
Droplet Mass Fraction (%)
2.0
1.0
0.0
100.0
200.0
300.0
Extinction Strain Rate (1/s)

Figure 4

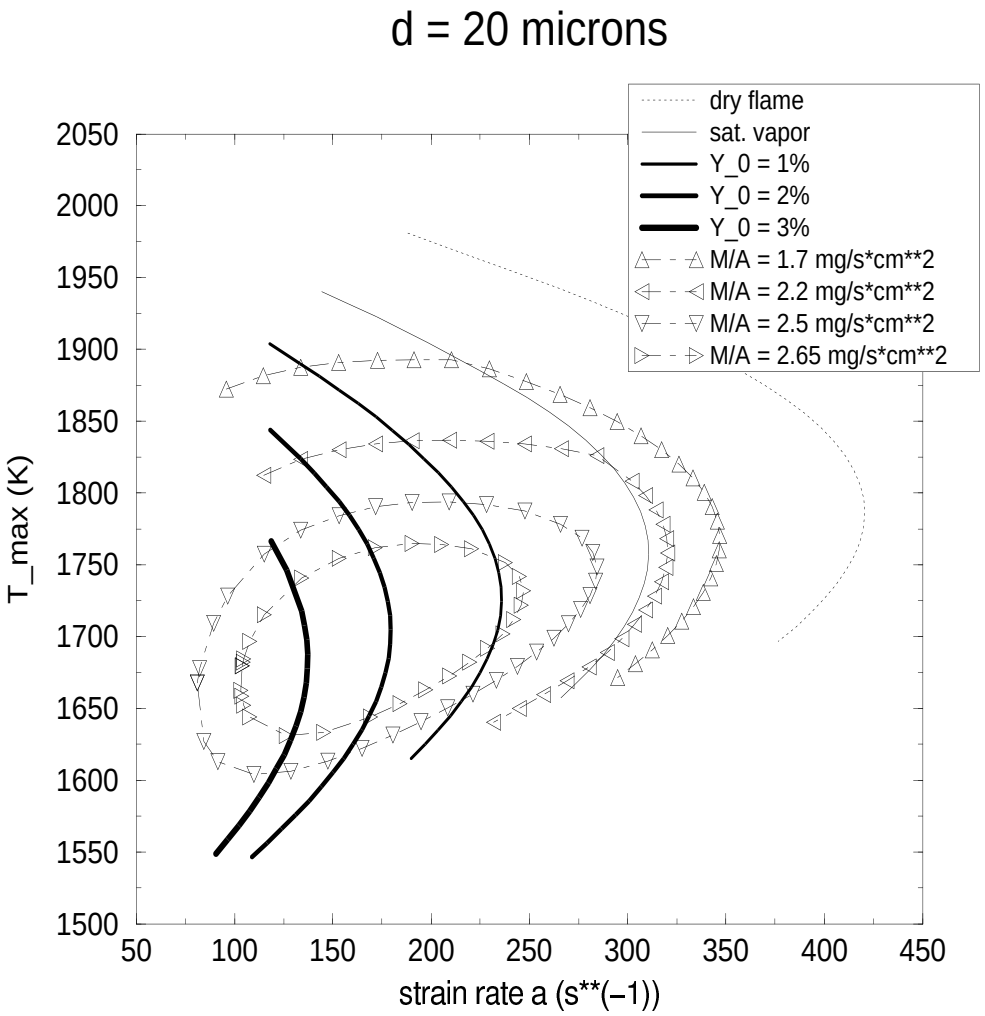
d = 20 microns
dry flame
sat. vapor
Y_0 = 1%
Y_0 = 2%
Y_0 = 3%
M/A = 1.7 mg/s*cm**2
M/A = 2.2 mg/s*cm**2
M/A = 2.5 mg/s*cm**2
M/A = 2.65 mg/s*cm**2
T_max (K)
2050
2000
1950
1900
1850
1800
1750
1700
1650
1600
1550
1500
50
100
150
200
250
300
350
400
450
strain rate a (s**(−1))

Figure 5